PHYSICAL REVIEW B **89**, 161102(R) (2014)

Coherent dynamics of photoinduced phase formation in a strongly correlated organic crystal

Yoshitaka Matsubara,[1] Sho Ogihara,[1] Jiro Itatani,[2] Nobuya Maeshima,[3,4] Kenji Yonemitsu,[5] Tadahiko Ishikawa,[1] Yoichi Okimoto,[1] Shin-ya Koshihara,[1,6] Takaaki Hiramatsu,[7] Yoshiaki Nakano,[8] Hideki Yamochi,[8] Gunzi Saito,[7] and Ken Onda[9,10,*]

[1]*Department of Chemistry and Materials Science, Tokyo Institute of Technology, O-okayama, Meguro-ku, Tokyo 152-8551, Japan*
[2]*Institute for Solid State Physics, The University of Tokyo, Kashiwanoha, Kashiwa, Chiba 277-8581, Japan*
[3]*Division of Materials Science, Faculty of Pure and Applied Sciences, University of Tsukuba, Tsukuba, Ibaraki 305-8573, Japan*
[4]*Center for Computational Sciences, University of Tsukuba, Tsukuba, Ibaraki 305-8577, Japan*
[5]*Department of Physics, Chuo University, Bunkyo-ku, Tokyo 112-8551, Japan*
[6]*CREST, Japan Science and Technology Agency (JST), O-okayama, Meguro-ku, Tokyo 152-8551, Japan*
[7]*Faculty of Agriculture, Meijo University, Tempaku-ku, Nagoya 468-8502, Japan*
[8]*Research Center for Low Temperature and Materials Sciences, Kyoto University, Sakyo-ku, Kyoto 606-8501, Japan*
[9]*Interactive Research Center of Science, Tokyo Institute of Technology, Nagatsuta, Midori-ku, Yokohama, Kanagawa 226-8502, Japan*
[10]*PRESTO, Japan Science and Technology Agency (JST), 4-1-8, Honcho, Kawaguchi, Saitama 332-0012 Japan*

(Received 19 July 2013; published 3 April 2014)

The photoinduced phase formation in a strongly correlated crystal $(EDO\text{-}TTF)_2PF_6$ (EDO-TTF: 4,5-ethylenedioxytetrathiafulvalene) is investigated using a 12 fs laser pulse. The formation time is determined as 40 fs with observation of coherence of electron-phonon coupled excited states prior to formation. The temperature-independent dephasing time is determined as ∼22 fs up to 180 K and the frequency of phonon oscillation is ∼38 THz, corresponding to the intramolecular vibrations in EDO-TTF. The phase formation is coherently controlled by relative-phase-controlled two-pulse excitation.

DOI: 10.1103/PhysRevB.89.161102 PACS number(s): 78.47.J−, 63.20.kd, 71.30.+h, 78.40.Me

Strongly correlated materials exhibit intriguing phases such as superconductor, Mott insulator, spin liquid, and charge density wave [1]. Competitions between electrons, phonons, and spins in the materials play a key role in creating these phases. Photoexcitation controls this competition and initiates cooperative response resulting in a macroscopic ordering, called photoinduced phase transition (PIPT). In PIPT, electron-phonon interactions lead to significant changes in dynamics. Thus, not only pure electronic but also electron-phonon dynamics have attracted considerable attention. Time-resolved optical spectroscopy has been widely used to study the electronic and vibrational dynamics and subsequent PIPT by monitoring the transient changes in optical constants on a femtosecond time scale [2–6]. However, the interactions dominating electronic phases are often inferred indirectly from these measurements.

Coherent nonlinear spectroscopy utilizing third-order nonlinear response is a powerful tool to directly investigate interactions and has been applied to reveal ultrafast dynamics in semiconductors [7,8], light-harvesting protein complexes [9–12], and other functional materials [13,14]. However, this spectroscopy has been applied only to a few strongly correlated materials [15] because their electronic coherence is considered to be too short owing to their strong electron-electron interaction. In this Rapid Communication we have investigated 10-fs time scale dynamics of the strongly correlated organic charge-transfer (CT) complex $(EDO\text{-}TTF)_2PF_6$ (EDO-TTF: 4,5-ethylenedioxytetrathiafulvalene) [16], which exhibits unique PIPT due to strong electron-phonon interactions. We also revealed the formation process of the photoinduced phase from the phonon-coupled excited state as well as the role of coherences in the excited state.

$(EDO\text{-}TTF)_2PF_6$ undergoes metal-insulator phase transition at 280 K because of its strong electron-electron and electron-phonon interactions and shows (0110)-type charge ordering below the transition temperature [16], where the number in parentheses represent the order of charge for EDO-TTF molecules, as shown in the upper panel of Fig. 1(a). This material exhibits a two-step phase transition triggered by photoexcitation in the low-temperature phase, that is, "insulator"–"photoinduced phase"–"metal" transition. The first step takes place within 100 fs and the photoinduced phase is assigned to the (1010) charge disproportionate phase, as shown in the lower panel of Fig. 1(a) [17–28]. The time required for the emergence of the metallic phase is 100 ps [22,23]. This distinctive PIPT is also considered to originate from its strong electron-phonon interaction [18,25].

A single crystal of $(EDO\text{-}TTF)_2PF_6$ was prepared according to a previously reported procedure [16]. Pump-probe spectroscopy was performed using a Ti:sapphire chirped-pulse amplifier (800 nm, 120 fs, 1 kHz) and a gas-filled hollow fiber (2.0 atm, krypton medium gas) to generate the broadband spectrum [29]. The broadband pulse was compressed using negative dispersion mirrors. The pulse width was estimated to be 12 fs from the cross correlation between the pump and probe pulses. The fluences of the pump and the probe pulses were set to 8.5 and 0.9 mJ/cm^2, respectively. It is noted that the PIPT dynamics is independent of fluence at this rate [20]. The polarization of the pump and probe pulse was set parallel to the stack direction of EDO-TTF molecules ($E \parallel a$).

Figure 1(b) presents the optical conductivity spectrum of $(EDO\text{-}TTF)_2PF_6$ in the low-temperature phase at 10 K along with the spectrum of the 12 fs laser pulse. The band at 1.37 eV is assigned to CT from the (0110) to (0200) and is designated

*onda.k.aa@m.titech.ac.jp

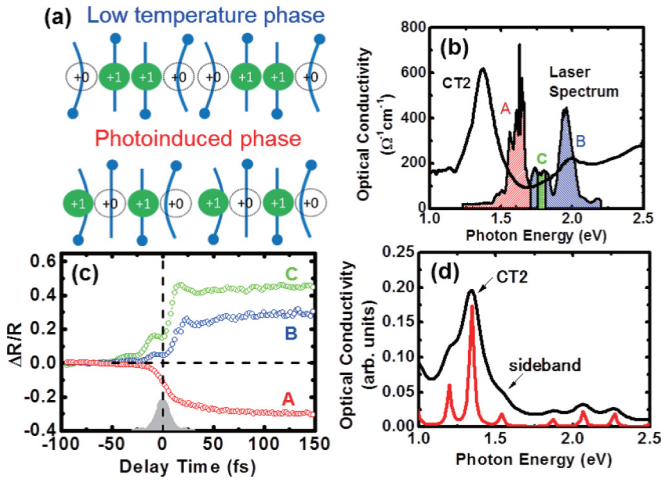

FIG. 1. (Color online) (a) Schematic diagram of charge distributions and EDO-TTF molecule deformation in the low-temperature phase and photoinduced phase of $(EDO\text{-}TTF)_2PF_6$. (b) Optical conductivity spectrum for the low-temperature phase of $(EDO\text{-}TTF)_2PF_6$ at 10 K (solid line) and the laser pulse spectrum (shaded area with solid line). Regions A (red), B (blue), and C (green) represent the three different detection regions of the probe pulse. (c) Temporal profiles for $\Delta R/R$ probed at regions A (red), B (blue), and C (green). The gray shaded area represents the cross-correlation profile of the pump and probe pulses. (d) Calculated spectrum considering the coupling between the CT2 excited state and intermolecular vibrations (see Supplementary Material for details [31]). The black and red lines show spectra with broadening factors of $\varepsilon/t_0 = 0.5$ and 0.1, respectively.

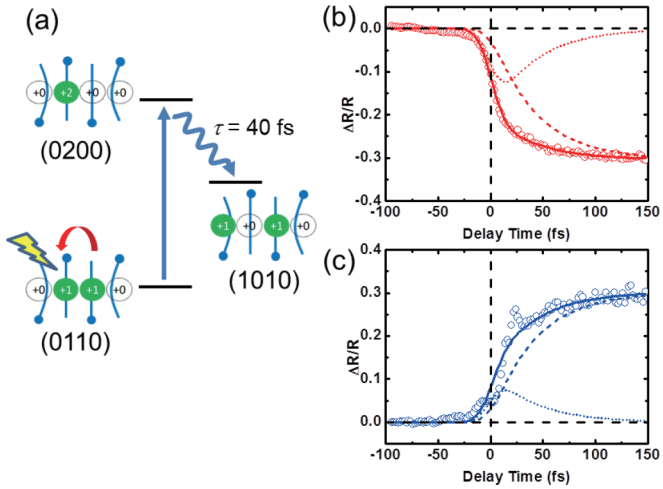

FIG. 2. (Color online) (a) Schematic illustration of the changes in charge distribution for the initial process of PIPT in $(EDO\text{-}TTF)_2PF_6$. (b) and (c) Experimental (circles) and simulated (solid lines) temporal profiles of $\Delta R/R$ probed at regions (b) A and (c) B. The dotted and dashed lines represent the first and second components in the fitting function, respectively.

as CT2 band [30]. Figure 1(c) shows the temporal profiles of the reflectivity changes ($\Delta R/R$) after photoexcitation of the low-temperature phase at 25 K. The red, blue, and green lines represent the temporal profiles of $\Delta R/R$ probed at photon energies <1.59 eV (region A), >1.59 eV (region B), and at ~ 1.65 eV (region C), respectively. These regions were selected from the reflected probe pulse with optical filters in front of the photodetector. The cross correlation of the pump and probe pulses is indicated by the gray shaded area. After photoexcitation, reflectivity decreases in region A and increases in regions B and C. These changes correspond to the disappearance of the CT2 band.

To analyze this temporal behavior, the model shown in Fig. 2(a) was adopted. Photoexcitation at ~ 1.55 eV creates the (0200) CT2 state [30], and the photoinduced (1010) phase then emerges [18]; thus we can assume an exponential transfer from the (0200) state to the (1010) phase, with a time constant τ [31]. Figures 2(b) and 2(c) compare the experimental data (open circles) with the fitting function (solid lines). The dotted and dashed lines represent the components of the (0200) CT2 state and (1010) photoinduced phase in the fitting function for regions A and B, respectively. The time constant obtained from the fitting is $\tau = 40 \pm 5$ fs, which is regarded as the formation time of the (1010) photoinduced phase from the (0200) CT2 excited state. The time scale of the CT processes deduced from the transfer integral $t = 0.16$ eV [25,30] is approximately $h/t = 26$ fs, which is less than the obtained formation time of ~ 40 fs. Therefore, it is concluded that the structural changes influence the formation of the photoinduced (1010) phase, and the electron-phonon interactions dominate the process.

The temporal profiles for regions B and C shown in Fig. 1(c) have apparent signals over 50 fs before time zero. This negative delay signal designated as perturbed free induction decay allows us to explore excited-state coherence. The excited-state coherence is typically investigated using third-order nonlinear process such as four-wave-mixing techniques [7,8]; however, it is difficult to find the four-wave mixing signals because the light is diffracted to a direction different from direction of the pump and probe pulses as follows:

$$k_{\mathrm{NL}} = 2k_{\mathrm{Pump(Probe)}} - k_{\mathrm{Probe(Pump)}}. \quad (1)$$

Here k_{NL}, k_{Pump}, and k_{Probe} are directions of the light diffracted by nonlinear process, the pump pulse, and the probe pulse, respectively. For negative delay signals, the probe precedes the pump pulse and produces a coherent polarization of the excited states, resulting in a weak signal starting before zero-time delay. Advantage of this process is that the conventional pump-probe configuration is applicable [32–34] because the direction of the diffracted light is the same as that of the probe light:

$$k_{\mathrm{NL}} = k_{\mathrm{Probe}} + k_{\mathrm{Pump}} - k_{\mathrm{Pump}} = k_{\mathrm{Probe}}. \quad (2)$$

As shown in the schematic energy diagram in Fig. 3(a), photon energy of the diffracted light in the negative delay region corresponds to the energy of the excited states. From this point, negative delay signal is caused by the coherence of the CT2 excited states because the photon energy of the detected light is ~ 1.6 eV. The distinct negative delay signals in region B and C suggest phonon-sideband arising from strong electron-phonon coupling as discussed later. In addition, lower reflectivity in regions B and C permits the detection of the negative delay signals.

The open green circles in Fig. 3(b) represent the magnified temporal profile of $\Delta R/R$ in region C, within the range of

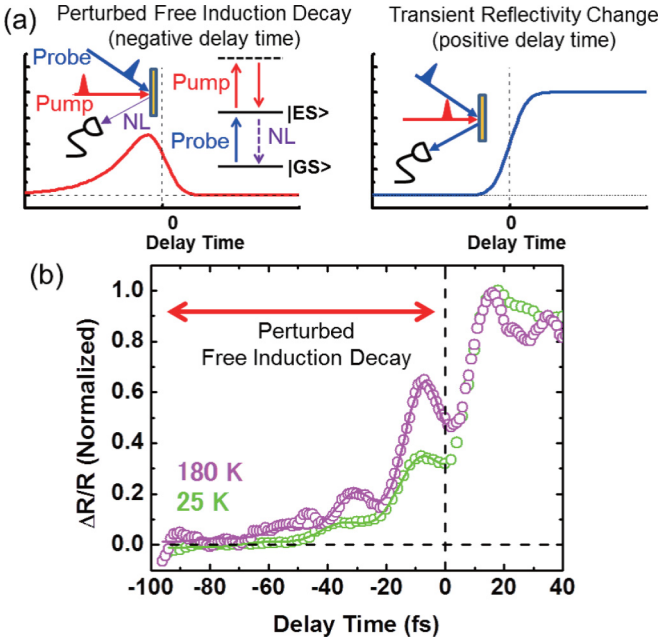

FIG. 3. (Color online) (a) Schematic diagram of the perturbed free induction decay in the negative delay time and the transient reflectivity change in the positive delay time. GS and ES notations correspond to the ground and excited states. NL indicates the light diffracted by the third-order nonlinear process. (b) Magnified view of the temporal profiles in the negative delay time probed in region C at 25 K (green circles) and at 180 K (pink circles). The solid lines indicate the fitting functions.

negative delay. The green solid line represents the fitting function composed of exponential function and damped oscillation. Although pure electronic excited states such as excitons [32,33] show simple exponential decay, phonon coupled electronic excited states such as polarons [34] exhibit oscillation due to the modulation by electron-phonon interactions. The obtained decay times for exponential and oscillating part were 22 ± 1 and 19 ± 1 fs, respectively. The oscillation frequency corresponding to coupled phonon was 38 ± 1 THz. The decay time of the exponential part corresponds to dephasing, which is affected by formation of the photoinduced phase. Hence the obtained dephasing time consists of two components as follows:

$$\frac{1}{T_2} = \frac{1}{2T_1} + \frac{1}{T_2'}. \tag{3}$$

Here T_2 is the experimentally obtained dephasing time, T_1 is the population decay time, and T_2' is the pure dephasing time without energy relaxation. From the value $T_1 = \tau = 40$ fs and $T_2 = 22$ fs, contributions of the first and second terms to the dephasing are 28% and 72%, respectively. Therefore, it is necessary to consider not only the photoinduced phase formation but also other interactions to explain the dephasing process.

Thermal motion of the lattice randomize phase of the excited-state wave function [7,8]. The pink open circles and solid line in Fig. 3(b) represent the experimental data and the fitting function at 180 K, respectively. The obtained dephasing time of the exponential function was $T_2 = 21 \pm 1$ fs, which is approximately that observed at 25 K. This result suggests that the possible origin of the dephasing is not lattice phonon [35,36] but electron-electron interactions [37].

Local optical phonons affect the dephasing to a lesser extent and modulate negative delay signals [8]. To date, coherent optical phonons in the positive delay signal have been often studied in PIPT in other materials [3,4]; however, it was difficult for these studies to distinguish coherent phonons in excited states from those in ground state by impulsive Raman excitation [34]. In contrast, since only excited states contribute to the negative delay signal, it implies that the observed oscillation couples to the CT2 states. On assessment of the frequency, the observed oscillation corresponds to the charge-sensitive intramolecular C=C vibrations (optical phonons) in EDO-TTF [30]. The oscillation is observed only in the negative delay, indicating that the vibration is coupled only to the CT2 excited states but not to the photoinduced state. Thus, it is considered that the coupling between the C=C vibrations and the CT2 excited states forms the precursor states of the photoinduced phase.

We conducted the calculation using a one-dimensional two-orbital Holstein-Hubbard model for considering the electron-phonon coupling [31]. Figure 1(d) shows the calculated optical conductivity spectrum, where the red and black lines are the broadened spectra with widths of $\varepsilon/t_0 = 0.5$ and 0.1, respectively. The black spectrum is in good agreement with the experimental spectrum. The red spectrum consists of three types of bands: CT2 at 1.37 eV, the intramolecular transition bands at ~2.0 eV, and their sidebands. This sideband emerges only when the coupling is sufficiently large. Although it is difficult to separate this sideband in the experimental spectrum owing to broad spectral widths, the pump pulse at ~1.55 eV excites mainly the CT2 band and the sideband just above the CT2 band. Hence, the sideband presumably leads to strong negative delay signal in regions B and C. Moreover, the previous time-dependent calculation predicted the delayed formation of the photoinduced phase accompanied by intramolecular vibrations, although the parameters in the model were not precise owing to the lack of experimental results for the initial process [18]. These theoretical results indicate that both lattice and local phonons play a key role, particularly, in the initial dynamics of PIPT.

The following information can be drawn from the above results. Photoexcitation of the charge localized (0110) phase directly creates the coupled coherence between the charge transfer excited states (CT2) and the charge sensitive C=C vibrations. Immediately after dephasing, the charge disproportionate (1010) phase is formed. In the recent study of 10-fs time scale dynamics in quasi-one-dimensional Mott insulator ET-F_2TCNQ [5], an oscillation with a frequency of $\sim V/h$ (V is the intersite Coulomb repulsion) arising from interference of bound and ionized holon-doublon excitation has been reported. Although this process is important in describing the 10-fs time scale dynamics, it is not consistent with our results, i.e., the frequency $V/h = 68$ THz [18] in $(EDO\text{-}TTF)_2PF_6$ is not consistent with the observed frequency of 38 THz. In addition, such interference is not expected in the previous theoretical study [18].

Using this unique and relatively long electronic coherence, we attempted to control formation of the photoinduced phase by interference of the wave functions [38–40] using a pump

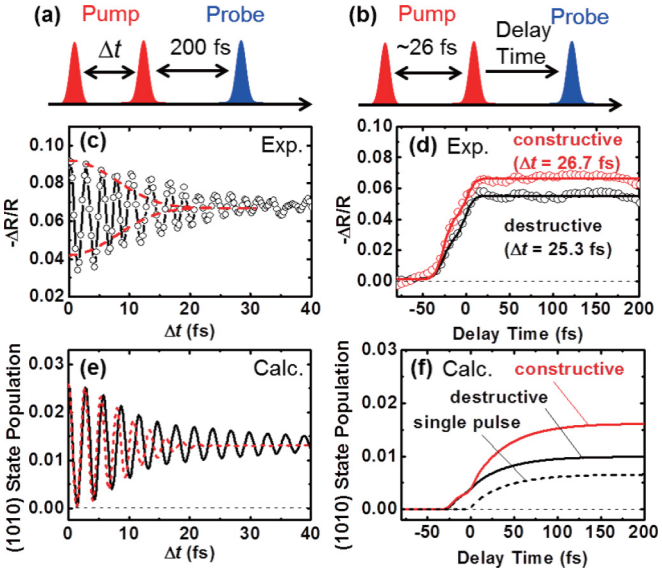

FIG. 4. (Color online) (a) and (b) Schematic illustrations of the pump and probe pulse sequences in the coherent control experiments. (c) The black circles and solid line represent profiles of $\Delta R/R$ measured using the sequence (a). The red dashed lines represent linear autocorrelation calculated from the second harmonic autocorrelation. (d) Temporal profiles of $\Delta R/R$ measured using the sequence (b). The red and black circles represent constructive and destructive excitations, respectively. (e) Calculated profiles of the photoinduced phase population assuming the sequence (a). The black solid and the red dashed lines represent the profiles assuming $T_2 = 26$ and 1 fs, respectively. (f) The calculated profiles of the photoinduced phase population assuming the sequence (b). The red and black solid lines represent the population of the photoinduced phase excited by constructive and destructive two-pulse excitations, respectively. The black dashed line represents the population excited by a single pulse.

pulse pair, whose relative phase is controlled by a Michelson interferometer [41]. Two measurements were performed: (1) $\Delta R/R$ measured as a function of the interval Δt between the pump pulses with a fixed delay time between the probe pulse and the second pump pulse [Fig. 4(a)], and (2) $\Delta R/R$ measured as a function of the delay time of the probe pulse with fixed Δt [Fig. 4(b)].

In Fig. 4(c), the black circles and solid line show the temporal profile of the measurement (1). The red dashed line represents linear autocorrelation calculated from second harmonic autocorrelation. The periodic modulation of $\Delta R/R$ with a period less than 3 fs indicates that the density of the photoinduced phase is affected by interference between the CT2 excited states produced by the first and second pump pulses. Figure 4(e) shows the calculated profiles of the photoinduced phase population at a fixed delay time of the probe pulse at 200 fs using density matrix equations [31]. In the model of the density matrix equations, we assume only the electronic states (ground state, CT2 excited state, and photoinduced phase) and neglect vibrational states as the contribution is negligible. The solid and dashed lines represent the profile for $T_2 = 26$ and 1 fs, respectively.

Figure 4(d) shows the temporal profiles of the measurement (2) with $\Delta t = 26.7$ fs for constructive excitation (red circles) or $\Delta t = 25.3$ fs for destructive excitation (black circles). The difference in temporal profiles for these excitations indicates how interference affects photoinduced phase generation. First, the difference in the generated density of the photoinduced phase was estimated on the basis of a phenomenological model, by assuming that the density of the photoinduced phase is expressed by the sum of the densities induced by the first and second pump pulses. The solid lines in Fig. 4(d) show the results of fitting with the function used in Fig. 2, indicating that 17% of the photoinduced phase generated by the first pump pulse was coherently controlled by the successive pulse.

Figure 4(f) shows calculated profiles. The solid lines represent the profile with $\Delta t = 26.8$ and 25.4 fs for constructive and destructive excitation, respectively. For reference, the profile for single pulse excitation is also included as the black dashed line. Comparing these profiles, it is concluded that 23% of the CT2 excited states are coherently manipulated.

In conclusion, the initial photoinduced dynamics in (EDO-TTF)$_2$PF$_6$ has been investigated using a compressed 12 fs optical pulse. A time constant of ~40 fs is determined for the formation of the photoinduced phase from the CT2 state. Immediately before the photoinduced phase formation, the coherence of the electron-phonon coupled precursor state can be observed as a negative delay signal. Here the dephasing with a time constant of ~22 fs accompanied with a 38 THz phonon oscillation which is assigned to the charge sensitive C=C vibrations. To the best of our knowledge, this is the first clear observation of the formation process of the photoinduced phase including excited-state coherence. By utilizing this coherence, approximately 17% of the photoinduced phase was successfully controlled using a relative-phase-controlled pulse pair. Our study extends the advancement for the development of all-optical control of electronic phases in materials within few femtoseconds.

This study was supported in part by a Grant-in-Aid for Scientific Research (B) (No. 20340074), Grants-in-Aid for Scientific Research on Innovative Areas (No. 21110512 and No. 20110006), the CREST and PRESTO programs of the Japan Science and Technology Agency (JST), and the G-COE program of the Tokyo Institute of Technology. Y.N. is indebted to the Chubei Itoh Foundation. We thank Dr. R. W. Schoenlein for his support in the initial stages of this work.

[1] D. N. Basov, R. D. Averitt, Dirk van der Marel, M. Dressel, and K. Haule, Rev. Mod. Phys. **83**, 471 (2011).

[2] M. Gonokami and S. Koshihara, J. Phys. Soc. Jpn. **75**, 011001 (2006).

[3] H. Uemura and H. Okamoto, Phys. Rev. Lett. **105**, 258302 (2010).
[4] Y. Kawakami, T. Fukatsu, Y. Sakurai, H. Unno, H. Itoh, S. Iwai, T. Sasaki, K. Yamamoto, K. Yakushi, and K. Yonemitsu, Phys. Rev. Lett. **105**, 246402 (2010).
[5] S. Wall, D. Brida, S. R. Clark, H. P. Ehrke, D. Jaksch, A. Ardavan, S. Bonora, H. Uemura, Y. Takahashi, T. Haseawa, H. Okamoto, G. Cerullo, and A. Cavalleri, Nat. Phys. **7**, 114 (2011).
[6] Y. Toda, T. Mertelj, T. Naito, and D. Mihailovic, Phys. Rev. Lett. **107**, 227002 (2011).
[7] D. S. Chemla and J. Shah, Nature (London) **411**, 549 (2001).
[8] S. T. Cundiff, Opt. Express **16**, 4639 (2008).
[9] J. M. Womick and A. M. Moran, J. Phys. Chem. B **113**, 15771 (2009).
[10] E. Collini, C. Y. Wong, K. E. Wilk, P. M. G. Curmi, P. Brumer, and G. D. Scholes, Nature (London) **463**, 644 (2010).
[11] G. Panitchayangkoon, D. Hayes, K. A. Fransted, J. R. Caram, E. Harel, J. Wen, R. E. Blankenship, and G. S. Engel, Proc. Natl. Acad. Sci. USA **107**, 12766 (2010).
[12] A. Ishizaki and G. R. Fleming, Annu. Rev. Condens. Matter Phys. **3**, 333 (2012).
[13] E. Collini and G. D. Scholes, Science **323**, 369 (2009).
[14] A. Nemeth, F. Miloa, J. Sperlng, D. Abramavicius, S. Mukamel, and H. F. Kauffmann, Chem. Phys. Lett. **469**, 130 (2009).
[15] K. D. Truong, P. Grenier, D. Houde, and A. D. Bandrauk, Chem. Phys. Lett. **196**, 280 (1992).
[16] A. Ota, H. Yamochi, and G. Saito, J. Mater. Chem. **12**, 2600 (2002).
[17] M. Chollet, L. Guerin, N. Uchida, S. Fukaya, H. Shimoda, T. Ishikawa, K. Matsuda, T. Hasegawa, A. Ota, H. Yamochi, G. Saito, R. Tazaki, S. Adachi, and S. Koshihara, Science **307**, 86 (2005).
[18] K. Onda, S. Ogihara, K. Yonemitsu, N. Maeshima, T. Ishikawa, Y. Okimoto, X. Shao,Y. Nakano, H. Yamochi, G. Saito, and Shin-ya Koshihara, Phys. Rev. Lett. **101**, 067403 (2008).
[19] K. Onda, S. Ogihara, T. Ishikawa, Y. Okimoto, X. Shao, Y. Nakano, H. Yamochi, G. Saito, and S. Koshihara, J. Phys. Conf. Ser. **148**, 012002 (2009).
[20] S. Ogihara, K. Onda, M. Shimizu, T. Ishikawa, Y. Okimoto, X. Shao, Y. Nakano, H. Yamochi, G. Saito, and S. Koshihara, J. Phys. Conf. Ser. **148**, 012008 (2009).
[21] J. Itatani, M. Rini, A. Cavalleri, K. Onda, T. Ishikawa, S. Ogihara, S. Koshihara, X. F. Shao, Y. Nakano, H. Yamochi, G. Saito, and R. W. Schoenlein, *Ultrafast Phenomena XVI* (Springer, Berlin, 2009), p.185.
[22] N. Fukazawa, M. Shimizu, T. Ishikawa, Y. Okimoto, S. Koshihara, T. Hiramatsu, Y. Nakano, H. Yamochi, G. Saito, and K. Onda, J. Phys. Chem. C **116**, 5892 (2012).
[23] M. Gao, C. Lu, H. Jean-Ruel, L. C. Liu, A. Marx, K. Onda, S. Koshihara, Y. Nakano, X. Shao, T. Hiramatsu, G. Saito, H. Yamochi, R. R. Cooney, G. Moriena, G. Sciaini, and R. J. D. Miller, Nature (London) **496**, 343 (2013).
[24] K. Onda, Y. Matsubara, T. Ishikawa, Y. Okimoto, S. Koshihara, T. Hiramatsu, G. Saito, Y. Nakano, G. Saito, and H. Yamochi, EPJ Web Conf. **41**, 03001 (2013).
[25] K. Yonemitsu and N. Maeshima, Phys. Rev. B **76**, 075105 (2007).
[26] M. Tsuchiizu and Y. Suzumura, Phys. Rev. B **77**, 195128 (2008).
[27] J. D. Lee, Phys. Rev. B **80**, 165101 (2009).
[28] K. Iwano and Y. Shimoi, Phys. Rev. Lett. **110**, 116401 (2013).
[29] M. Nisoli, S. De Silvestri, and O. Svelto, Appl. Phys. Lett. **68**, 2793 (1996).
[30] O. Drozdova, K. Yakushi, K. Yamamoto, A. Ota, H. Yamochi, G. Saito, H. Tashiro, and D. B. Tanner, Phys. Rev. B **70**, 075107 (2004).
[31] See Supplemental Material at http://link.aps.org/supplemental/10.1103/PhysRevB.89.161102 for details of the calculations.
[32] M. Joffre, D. Hulin, A. Migus, A. Antonetti, C. B. à la Guillaume, N. Peyghambarian, M. Lindberg, and S. W. Koch, Opt. Lett. **13**, 276 (1988).
[33] F. Sotier, T. Thomay, T. Hanke, J. Korger, S. Mahapatra, A. Frey, K. Brunner, R. Bratschitsch, and A. Leitenstorfer, Nat. Phys. **5**, 352 (2009).
[34] T. Kobayashi, J. Du, W. Feng, and K. Yoshino, Phys. Rev. Lett. **101**, 037402 (2008).
[35] L. Schultheis, J. Kuhl, A. Honold, and C. W. Tu, Phys. Rev. Lett. **57**, 1797 (1986).
[36] L. Schultheis, A. Honold, J. Kuhl, K. Köhler, and C. W. Tu, Phys. Rev. B **34**, 9027 (1986).
[37] P. C. Becker, H. L. Fragnito, C. H. B. Cruz, R. L. Fork, J. E. Cunningham, J. E. Henry, and C. V. Shank, Phys. Rev. Lett. **61**, 1647 (1988).
[38] T. Kampfrath, A. Sell, G. Klatt, A. Pashkin, S. Mährlein, T. Dekorsy, M. Wolf, M. Fiebig, A. Leitenstorfer, and R. Huber, Nat. Photon. **5**, 31 (2011).
[39] A. P. Heberle, J. J. Baumberg, and K. Kohler, Phys. Rev. Lett. **75**, 2598 (1995).
[40] S. Iwai, Y. Ishige, S. Tanaka, Y. Okimoto, Y. Tokura, and H. Okamoto, Phys. Rev. Lett. **96**, 057403 (2006).
[41] N. F. Scherer, R. J. Carlson, A. Matro, M. Du, A. J. Ruggiero, V. Romero-Rochin, J. A. Cina, G. R. Fleming, and S. A. Rice, J. Chem. Phys. **95**, 1487 (1991).